Single-frequency 571 nm VECSEL for photoionization of magnesium

S. C. Burd[a], T. Leinonen[b], J. P. Penttinen[b], D. T. C. Allcock[a], D. H. Slichter[a], R. Srinivas[a], A. C. Wilson[a], M. Guina[b], D. Leibfried[a], and D. J. Wineland[a]

[a]Time and Frequency Division, National Institute of Standards and Technology, 325 Broadway, Boulder, Colorado, 80305, USA

[b]Optoelectronics Research Centre, Tampere University of Technology, PO Box 692, FIN-33101 Tampere, Finland

ABSTRACT

We report the development of an intracavity-frequency-doubled vertical external-cavity surface-emitting laser (VECSEL) emitting at 571 nm for photoionization of magnesium. The laser employs a V-cavity geometry with a gain chip at the end of one cavity arm and a lithium triborate (LBO) crystal for second harmonic generation. The gain chip has a bottom-emitting design with ten GaInAs quantum wells of 7 nm thickness, which are strain compensated by GaAsP. The system is capable of producing up to 2.4 ± 0.1 W (total power in two separate output beams) in the visible. The free-running relative intensity noise was measured to be below -55 dBc/Hz over all frequencies from 1 Hz to 1 MHz. With acoustic isolation and temperature regulation of the laser breadboard, the mode-hop free operation time is typically over 5 hrs. To improve the long-term frequency stability, the laser can be locked to a Doppler-free transition of molecular iodine. To estimate the short-term linewidth, the laser was tuned to the resonance of a reference cavity. From analysis of the on-resonance Hänsch-Couillaud error signal we infer a linewidth of 50 ± 10 kHz. Light at 285 nm is generated with an external build-up cavity containing a β-barium borate (BBO) crystal. The UV light is used for loading ^{25}Mg$^+$ ions in a surface-electrode RF Paul trap. These results demonstrate the applicability and versatility of high-power, single-frequency VECSELs with intracavity harmonic generation for applications in atomic and molecular physics.

Keywords: VECSEL, OPSL, SDL, frequency doubling, SHG, ion trapping, single-frequency, photoionization, Doppler-free spectroscopy, magnesium

1. INTRODUCTION

Trapped ions provide a versatile experimental platform for research in quantum information,[1–4] simulation[5–8] and fundamental quantum physics.[9] To trap ions, a source of neutral atoms must first be ionized. Electron bombardment[10] and laser photoionization[11] have been used for generating magnesium ions. The energy levels relevant for photoionization of magnesium are shown in Fig. 1. The ionization energy is 7.646 eV, corresponding to a deep-UV wavelength of 162.2 nm.[11] For ion trapping applications, it is more convenient to use a two-photon ionization scheme. Light from the photoionization (PI) laser, near resonance with the $^1S_0 \rightarrow {}^1P_1$ transition of neutral magnesium at 285.2 nm, excites a fraction of the population into the $^1P_1$ state. Photons from the PI laser or from another laser near 280 nm (used for Doppler of cooling Mg$^+$ ions) then have sufficient energy to excite the electron to the continuum, ionizing the atom. The natural linewidth of the $^1S_0 \rightarrow {}^1P_1$ transition is 80 MHz.[11]

Traditionally, frequency-doubled traveling-wave dye lasers have been used to generate 285 nm light.[11] An alternative is a master-oscillator power-amplifier (MOPA) system, where a low-power, single-frequency seed laser at 1140 nm is amplified with a Raman fiber amplifier[12] or a semiconductor tapered amplifier.[13] The output is then externally frequency quadrupled to 285 nm, with two sequential stages of second-harmonic generation.

Further author information: (Send correspondence to S.C.B)
S.C.B.: E-mail: shaun.burd@nist.gov, Telephone: (303) 497 5783

Widely-tunable optical parametric oscillators (OPOs) can also be used, but a single-frequency pump source in required. More recently, vertical external-cavity surface-emitting lasers (VECSELs) have been considered to exhibit advantageous properties for applications in photoionization and high-precision spectroscopy.[14] The VECSEL architecture allows single-frequency emission with close to diffraction-limited output beams and a tuning range of tens of nanometers. The semiconductor gain medium can be designed for direct emission over a broad wavelength range with demonstrations at 390 nm,[15] and at multiple wavelengths from around 650 nm[16] to 5.0 µm.[15] A larger range of wavelengths in the visible and UV (where there are a variety of relevant atomic transitions[14]) can be accessed through nonlinear conversion. Previously, externally-frequency-quadrupled VECSELs have been employed for Doppler-free spectroscopy of neutral mercury.[17] Here we show that for applications in atomic and molecular physics, VECSEL systems utilizing intra-cavity second harmonic generation offer a simpler, power-scalable alternative to laser sources relying exclusively on external harmonic generation. In this work we present an intracavity-frequency-doubled VECSEL emitting at 571 nm which is externally doubled to 285 nm for photoionization of magnesium. We show that the system has sufficient power for loading multiple ions and demonstrate that it exceeds the frequency stability requirements for isotope-selective photoionization of magnesium.
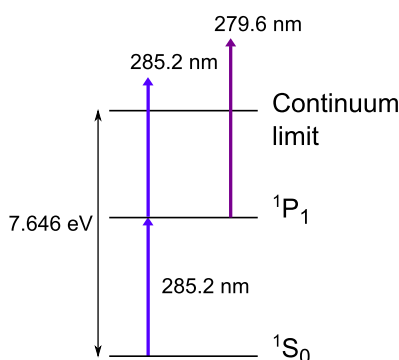

Figure 1. Energy levels relevant for photoionization of magnesium atoms. Direct excitation to the continuum requires photons of energy greater than 7.646 eV. In the two-photon ionization scheme, light from the photoionization (PI) laser at 285.2 nm excites a neutral Mg atom from the ground $^1S_0$ state to the $^1P_1$ state. Photons from the PI laser or 279.6 nm photons from a Mg^+ ion Doppler cooling laser serve to excite the atom from the $^1P_1$ state to the continuum.

2. GAIN MIRROR DESIGN

The design of the monolithic gain mirror is shown in Fig. 2. The structure was grown by solid-source molecular beam epitaxy (MBE) in reverse order, that is, the window layer was grown first, followed by the active region, and finally the distributed Bragg reflector (DBR) layers. The active region is composed of a lattice-matched GaInP window layer that also acts as an etch-stop layer. There are 10 GaInAs/GaAs quantum wells and 10 GaAsP strain-compensation layers located between the quantum wells. The 7 nm-thick quantum wells are located at the antinodes of the optical standing wave, whereas the strain compensation layers are situated at the nodes of the standing wave. The active region thickness was designed to be antiresonant at the signal wavelength to not produce a resonant microcavity in the gain chip. The DBR consists of 23.5 pairs of alternating AlAs/GaAs layers. For efficient heat extraction, the gain mirror is bonded from the DBR back surface onto a diamond heat spreader grown by chemical vapor deposition (CVD). The diamond heat spreader is attached to a copper mount for temperature control. A more detailed description of the gain chip is given by Kantola *et. al.* (2014).[18]

3. LASER SETUP

The laser cavity is shown in Fig. 3. A thermoelectric cooler (TEC) module is clamped between the gain mirror mount and a water-cooled, micro-channel cooler for thermal management and temperature control of the gain mirror. The gain mirror is pumped with a multimode diode laser at 807 nm with 40 W maximum power. The pump light is fiber coupled and focused onto the gain mirror with a $1/e^2$ intensity diameter of approximately 380 µm. The resonator has a standing-wave, V-cavity geometry consisting of the gain mirror, a 100 mm radius
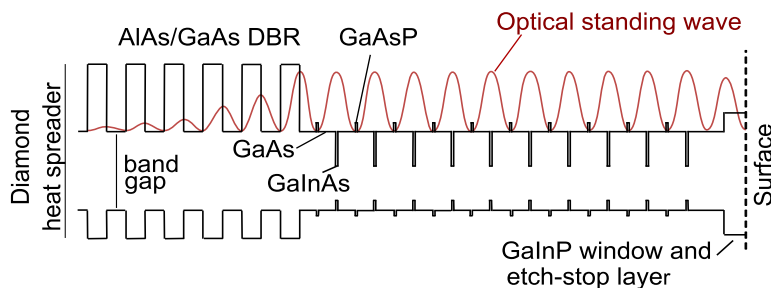
Figure 2. Gain mirror structure with an active region consisting of ten GaInAs/GaAs quantum wells strain compensated by GaAsP. The vertical axis is a qualitative measure of band-gap energy. DBR-Distributed Bragg reflector.
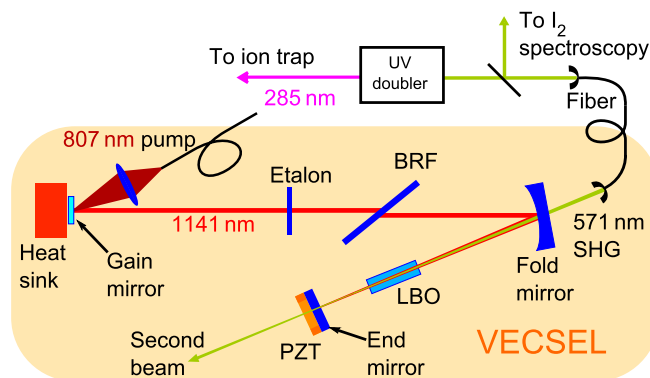

Figure 3. Intracavity-frequency-doubled VECSEL photoionization system. A 1141 nm standing wave is generated in a V-cavity consisting of the gain mirror, a 100 mm radius of curvature fold mirror and a flat end mirror. Light at 571 nm is generated using a 15 mm-long lithium triborate (LBO) crystal. A birefringent filter (BRF), etalon and piezo transducer (PZT) are used for frequency tuning. The output at 571 nm is transmitted through the cavity mirrors, fiber coupled, and directed to a resonant doubling cavity for generation of 285 nm light for photionization of magnesium. A portion of the output is used for Doppler-free spectroscopy of molecular iodine.

of curvature (ROC) folding mirror, and a plane end mirror. The folding mirror and end mirror are coated for high reflectivity (R>99.9 %) over the wavelength range 1116 nm-1142 nm and for high transmission at the corresponding second harmonic. Light at 571 nm leaves the cavity in two separate beams of roughly equal power. The end mirror is placed on a ring piezo transducer (PZT) to control the laser frequency. A 3 mm-thick quartz birefringent filter plate, inserted at Brewster's angle, and a 1 mm-thick yttrium aluminum garnet (YAG) etalon, are placed in the 125 mm long arm of the cavity for wavelength selection. A $3 \times 3 \times 15$ mm lithium triborate (LBO) crystal with anti-reflection coatings over 1116-1142 nm and 558-571 nm, cut for type-I critical phase matching, is placed in the 65 mm short arm of the cavity for second-harmonic generation. The etalon and LBO crystal are placed in mechanically stable, temperature-controlled ovens. We note that good temperature control (to within 0.05 °C) and mechanical stability of the LBO crystal are essential for stable, single-frequency operation of the laser. With a previous, less-rigid oven design, the laser would chaotically mode hop to other longitudinal modes and also to nearby etalon pass bands, rendering the laser useless for precision spectroscopy. The chaotic behavior was likely due to coupling of different longitudinal modes through sum-frequency generation in the LBO (also known as the "green problem"[19]). To reduce long-term frequency drifts due to thermally induced changes in the cavity length, the temperature of the laser's stainless steel breadboard is controlled (to within 0.05°C at the position of the temperature sensor) using alumina ceramic heaters.
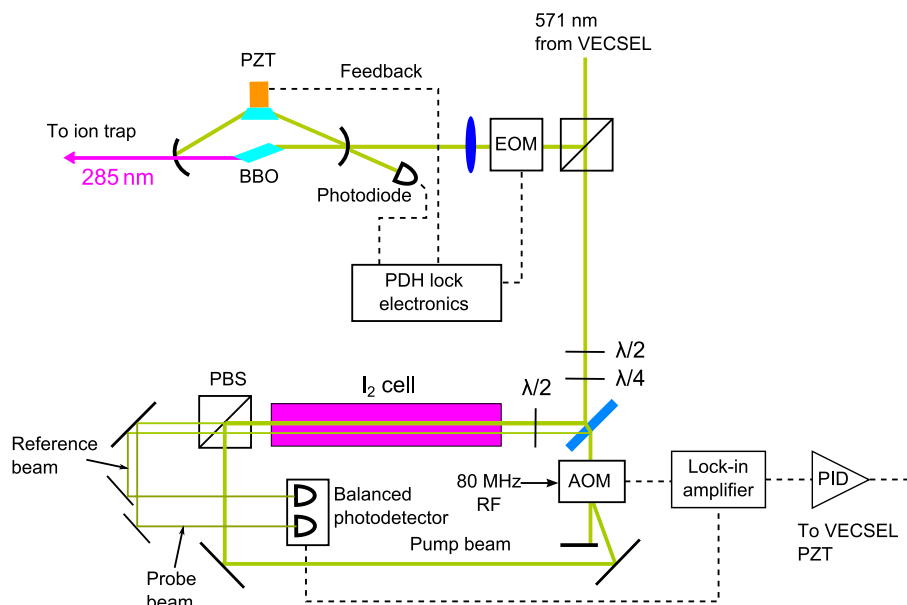
Figure 4. Setup for frequency doubling to the UV and modulation-transfer spectroscopy of molecular iodine. An electro-optic modulator (EOM) phase modulates the beam incident on the doubling cavity for Pound-Drever-Hall (PDH) locking. A portion of the light from the VECSEL is directed to the iodine lock setup. The beam is split into a strong pump beam, a probe and, a reference beam. An acousto-optic modulator (AOM) introduces a frequency shift between the pump and probe beams. A polarizing beam splitter (PBS) and a half-wave ($\lambda/2$) plate allow the pump and probe beams to overlap and counter propagate through the cell. A proportional-integral-derivative (PID) controller adjusts the laser cavity PZT to keep the cavity on resonance with the iodine line center.

For frequency doubling to 285 nm, a commercial doubling cavity (Spectra-Physics WaveTrain external cavity frequency doubler*) with a β-barium borate (BBO) crystal is utilized as shown in Fig. 4. An electro-optic modulator (EOM) is used to phase modulate the light entering the doubling cavity. The Pound-Drever-Hall technique is used to generate an error signal for locking the cavity to the laser.[22]

For long-term frequency stabilization we use a Doppler-free iodine spectrometer as shown in Fig. 4. The error signal, suitable for line peak locking, is generated using modulation-transfer spectroscopy.[20] An acousto-optic modulator (AOM) is used to shift the frequency of the pump beam by 80 MHz. This frequency offset eliminates the background signal resulting from interference between leakage pump light and the probe beam.[21] The 80 MHz signal is dithered at 100 kHz to provide frequency modulation for lock-in detection.

4. OUTPUT POWER AND INTENSITY NOISE

The output power of the laser, for different incident values of the 807 nm pump diode power, is shown Fig. 5. The data were recorded with the gain chip temperature set to 13°C and the laser frequency tuned to 525.405±0.001 THz (half the frequency required for excitation of the $^1S_0 \rightarrow {}^1P_1$ transition in magnesium). The 571 nm power plotted is the total output power in both second harmonic beams. Above a pump power of 15.2 W, corresponding to 980 ± 40 mW at 571 nm, thermal rollover is evident and the laser power starts to decrease. Reducing the pump power below 11.5 W, induces mode hopping. The output power has also been measured with a gain chip temperature of 8°C. At the lower temperature, the laser can generate up to 2.4 ± 0.1 W (total power

---

*Commercial equipment, instruments, and materials are identified in this paper in order to specify the experimental procedure accurately. Such identification does not imply recommendation or endorsement by the National Institute of Standards and Technology, nor is it intended to imply that the materials or equipment identified are necessarily the best available for the purpose.
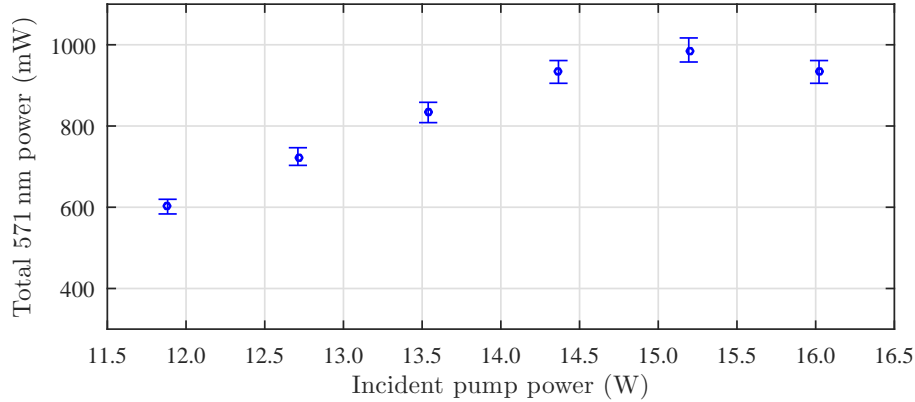
Figure 5. Laser output power at 525.405±0.001 THz as a function of pump diode power incident on the gain chip. The gain chip temperature was set to 13 °C. The error bars include the calibration uncertainty of the power meter.
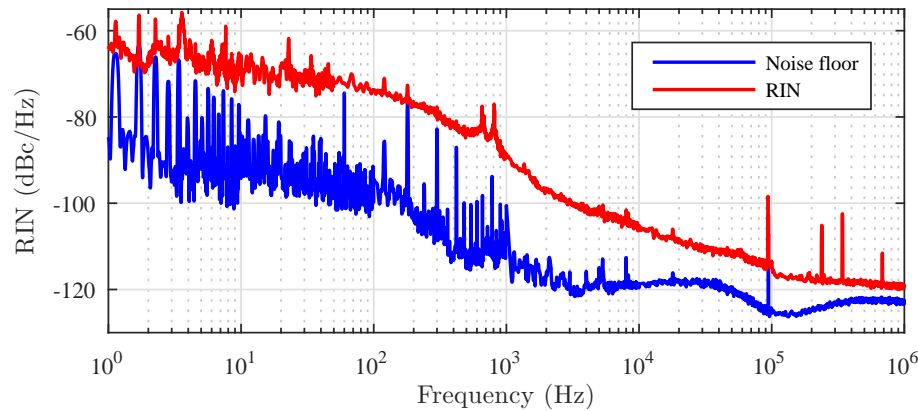

Figure 6. Relative intensity noise power spectral density for operation at 0.93 W total output power at 571 nm.

in both output beams) of 571 nm light with a pump power of 18.5 W. However, to avoid condensation of water on the gain mirror, we generally operate the laser at 13°C.

The relative intensity noise (RIN) of the free-running laser (without active frequency stabilization) is given is Fig. 6. The RIN was measured using the basic system described by Obarski and Splett.[23] The experiment was performed using a photodiode with a specified 5.5 MHz bandwidth connected to a fast Fourier transform analyzer. The noise is less than -55 dB/Hz over the entire frequency range. The strong features near 700 Hz are probably due to acoustic noise in the lab and vibrations from the water cooling system. The noise spikes around 500 kHz are thought to be due to switching noise in the current supply of the pump diode.

5. FREQUENCY STABILIZATION

The laser frequency was recorded over several hours using a wavemeter with an absolute accuracy of 600 MHz. Without stabilization of the breadboard to within 0.05 °C, the laser frequency drifts at a rate of roughly 0.2 GHz/min, resulting in mode hops approximately every 15 minutes. Temperature stabilization of the laser breadboard typically enables a mode-hop-free operation time of at least 5 hours. To further reduce slow frequency drifts, the laser can be locked to a Doppler-free molecular iodine line using the spectrometer shown in Figure 4. Fig. 7 shows a Doppler-free spectrum of the iodine lines near 525.5040 THz. The frequency axis of the spectrum was calibrated using the software IodineSpec5.[24] The zero detuning point is the center of the line which is used for the lock error signal. A more detailed scan of this line is given in Fig 8 (a). The gradient of the error signal at the lock point was used to estimate the slow frequency fluctuations from the locked error signal. Fig. 8 (b) shows the locked error signal recorded for more than 6 minutes. The standard deviation of the error signal from the lock point is 90 kHz. The closed-loop servo bandwidth was estimated to be 160 Hz. To estimate
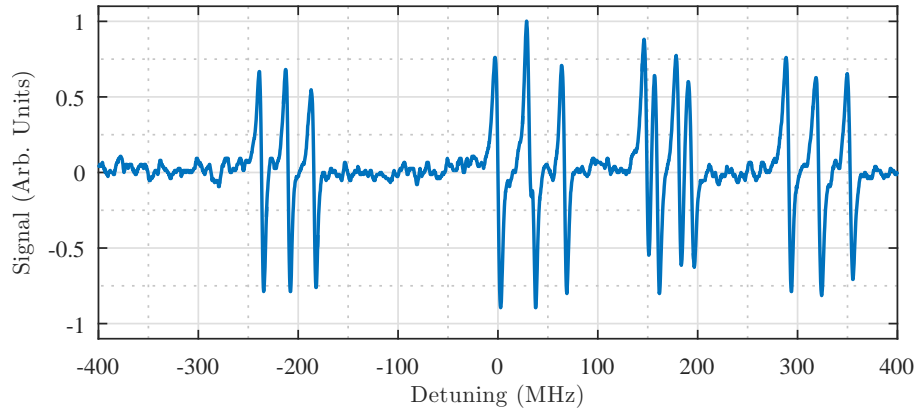
Figure 7. Doppler-free spectrum of molecular iodine relative to 525.4050 THz. The lock-in amplifier time constant was 10 ms.
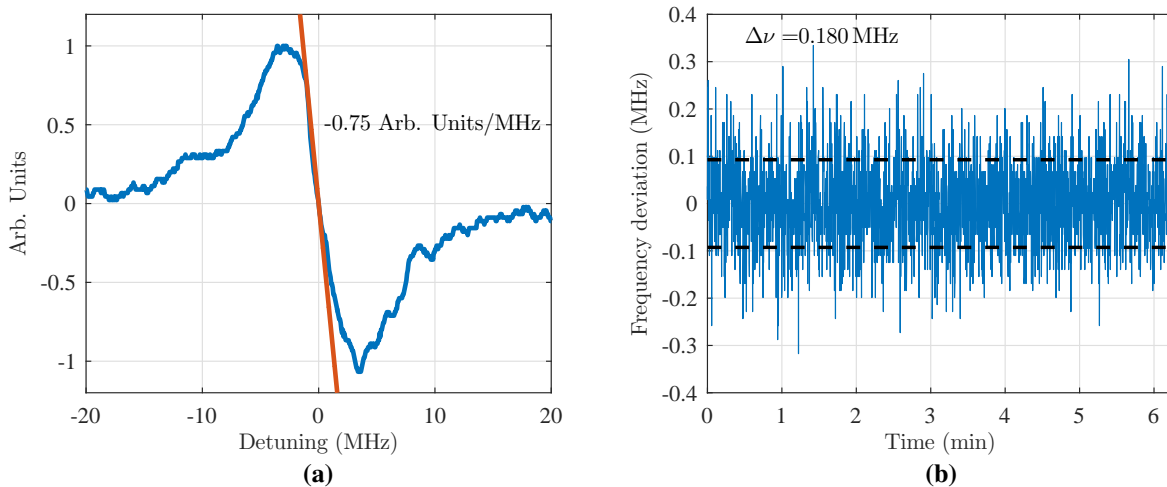

Figure 8. a) Zoomed in spectrum of the iodine error signal used for locking. The lock-in time constant was 1 ms. The orange line indicates the slope of the error signal at the lock point with a value of -0.75 Arb. Units/MHz b) Locked error signal. The dashed black lines indicate a standard deviation above and below the lock point. With a servo bandwidth of roughly 160 Hz, twice the standard deviation, $\Delta\nu = 180$ kHz.

the laser linewidth on shorter time scales, the laser was tuned to the resonance frequency of a reference cavity with a free spectral range of 450 ± 6 MHz and a finesse of 250 ± 10. The Hänsch-Couillaud (HC) method[25] was used to generate an error signal giving a measure of the laser's frequency fluctuations. Analysis of the error signal gives a linewidth of 50 ± 10 kHz with a detector bandwidth of 0.47 MHz.

6. PHOTO-IONIZATION

In our magnesium ion trapping apparatus, a thermal beam of ^{25}Mg isotopically enriched neutral atoms is produced with an electrically heated oven. Light at 285 nm from the external doubling cavity is coupled into a single-mode solarization resistant UV fiber[26] and focused to a $1/e^2$ intensity diameter of approximately 26 μm through the potential minimum of a surface-electrode RF Paul trap similar to that described by Ospelkaus et. al.[27] Roughly 1 mW of power is used. Light at 279.6 nm for Doppler cooling (either from a frequency-quadrupled fiber laser system or a frequency-quadrupled VECSEL system) is also applied to the trap center. After allowing the oven to reach a temperature high enough to develop a significant flux of neutral Mg, we reliably and repeatably load single Mg ions into the trap within 10 s. Fig. 9 shows a EMCCD photograph of two ^{25}Mg$^+$ ions that were loaded using the intracavity-frequency-doubled VECSEL system.

Figure 9. EMCCD image of two trapped ^{25}Mg$^+$ ions loaded into a surface-electrode RF-Paul trap.

7. CONCLUSION

We present a single-frequency 571 nm source derived from an intracavity-frequency-doubled VECSEL with sufficiently low frequency and intensity noise for performing high-resolution atomic and molecular spectroscopy. The system is incorporated in a magnesium ion trapping setup and is used in free running mode for non-isotopically selective photoionization of magnesium atoms. The laser can be used for performing Doppler-free spectroscopy of molecular iodine and can be stabilized to a Doppler-free transition. Since the $\sim$10 MHz width of the iodine features is substantially narrower than the 80 MHz natural linewidth of the ^{1}S$_0 \to \,^1$P$_1$ transition of neutral magnesium, it should also be possible to use the system for isotope-selective photoionization. The low frequency and intensity noise of our system suggest that high-power, intracavity-frequency-doubled VECSELs could be used for other laser tasks in atomic and molecular physics such as Doppler cooling, quantum state manipulation with stimulated-Raman transitions and cooling to the motional ground state.

ACKNOWLEDGMENTS

REFERENCES

[1] Leibfried, D., Blatt, R., Monroe, C., and Wineland, D. J., "Quantum dynamics of single trapped ions," *Rev. Mod. Phys.* **75**, 281–324 (Mar 2003).

[2] Cirac, J. I. and Zoller, P., "Quantum computations with cold trapped ions," *Phys. Rev. Lett.* **74**, 4091–4094 (May 1995).

[3] Steane, A., "The ion trap quantum information processor," *Appl. Phys. B* **64**(6), 623–642 (1997).

[4] Blatt, R. and Wineland, D. J., "Entangled states of trapped atomic ions," *Nature* **453**(108-1015) (2008).

[5] Britton, J. W., Sawyer, B. C., Keith, A. C., Wang, C. C. J., Freericks, J. K., Uys, H., Biercuk, M. J., and Bollinger, J. J., "Engineered two-dimensional Ising interactions in a trapped-ion quantum simulator with hundreds of spins," *Nature* **484**, 489–492 (2012).

[6] Blatt, R. and Roos, C. F., "Quantum simulations with trapped ions," *Nature Physics* **8**, 277–284 (2012).

[7] Monroe, C., Campbell, W. C., Edwards, E. E., Islam, R., Kafri, D., Korenblit, S., Lee, A., Richerme, P., Senko, C., and Smith, J., "Quantum simulation of spin models with trapped ions," in [*Proceedings of the International School of Physics 'Enrico Fermi', Course 189*], Knoop, M., Marzoli, I., and Morigi, G., eds., 169–187 (2015).

[8] Schneider, C., Porras, D., and Schaetz, T., "Experimental quantum simulations of many-body physics with trapped ions," *Rep. Prog. Phys.* **75**, 024401 (2012).

[9] Kotler, S., Akerman, N., Navon, N., Glickman, Y., and Ozeri, R., "Measurement of the magnetic interaction between two bound electrons of two separate ions," *Nature* **510**, 376–380 (2014).

[10] Wineland, D. J., Monroe, C., Itano, W. M., Leibfried, D., King, B. E., and Meekhof, D. M., "Experimental issues in coherent quantum-state manipulation of trapped atomic ions," *J. Res. Nat. Inst. Stand. Technol.* **103**(3), 259–328 (1998).

[11] Madsen, D. N., Balslev, S., Drewsen, M., Kjærgaard, N., Videsen, Z., and Thomsen, J. W., "Measurements on photo-ionization of $3s3p^1P_1$ magnesium atoms," *J. Phys. B: At. Mol. Opt. Phys.* **33**(22), 4981–4988 (2000).

[12] Feng, Y., Taylor, L. R., and Calia, D. B., "150 W highly-efficient Raman fiber laser," *Opt. Express* **17**, 23678–23683 (2009).

[13] Zhang, J., Yuan, W. H., Deng, K., Deng, A., Xu, Z. T., Qin, C. B., Lu, Z. H., and Luo, J., "A long-term frequency stabilized deep ultraviolet laser for Mg^+ ions trapping experiments," *Rev. Sci. Instrum.* **84**(12) (2013).

[14] Burd, S. C., Leibfried, D., Wilson, A. C., and Wineland, D. J., "Optically pumped semiconductor lasers for atomic and molecular physics," *Proc. SPIE* **9349**, 93490P (2015).

[15] Kuznetsov, M., "VECSEL semiconductor lasers: A path to high-power, quality beam and UV to IR wavelength by design," in [*Semiconductor Disk Lasers: Physics and Technology*], Okhotnikov, O. G., ed., ch. 1, 1, Wiley-VCH (2010).

[16] Calvez, S., Hastie, J. E., Guina, M., Okhotnikov, O. G., and Dawson, M. D., "Semiconductor disk lasers for the generation of visible and ultraviolet radiation," *Laser and Photonics Reviews* **3**(5), 407–434 (2009).

[17] Paul, J., Kaneda, Y., Wang, T.-L., Lytle, C., Moloney, J. V., and Jones, R. J., "Doppler-free spectroscopy of mercury at 253.7 nm using a high-power, frequency-quadrupled, optically pumped external-cavity semiconductor laser," *Opt. Lett.* **36**(1), 61–63 (2011).

[18] Kantola, E., Leinonen, T., Ranta, S., Tavast, M., and Guina, M., "High-efficiency 20 W yellow VECSEL," *Opt. Express* **22**(6), 6372–6380 (2014).

[19] Baer, T., "Large-amplitude fluctuations due to longitudinal mode coupling in diode-pumped intracavity-doubled Nd:YAG lasers," *J. Opt. Soc. Am. B* **3**, 1175–1180 (Sep 1986).

[20] Shirley, J. H., "Modulation transfer processes in optical heterodyne saturation spectroscopy," *Opt. Lett.* **7**, 537–539 (Nov 1982).

[21] Snyder, J. J., Raj, R. K., Bloch, D., and Ducloy, M., "High-sensitivity nonlinear spectroscopy using a frequency-offset pump," *Opt. Lett.* **5**, 163–165 (Apr 1980).

[22] Drever, R., Hall, J., Kowalski, F., Hough, J., Ford, G., Munley, A., and Ward, H., "Laser phase and frequency stabilization using an optical resonator," *Applied Physics B* **31**(2), 97–105 (1983).

[23] Obarski, G. E. and Splett, J. D., "Transfer standard for the spectral density of relative intensity noise of optical fiber sources near 1550 nm," *J. Opt. Soc. Am. B* **18**(6) (2001).

[24] Knockel, H. and Tiemann, E., "Iodinespec," (2013). http://www.iqo.uni-hannover.de (2013).

[25] Hänsch, T. and Couillaud, B., "Laser frequency stabilization by polarization spectroscopy of a reflecting reference cavity," *Opt. Commun.* **35**, 441–444 (1980).

[26] Colombe, Y., Slichter, D. H., Wilson, A. C., Leibfried, D., and Wineland, D. J., "Single-mode optical fiber for high-power, low-loss UV transmission," *Opt. Express* **22**, 19783–19793 (Aug 2014).

[27] Ospelkaus, C., Warring, U., Colombe, Y., Brown, K. R., Amini, J. M., Leibfried, D., and Wineland, D. J., "Microwave quantum logic gates for trapped ions," *Nature* **476**, 181–184 (2011).